Supporting Information

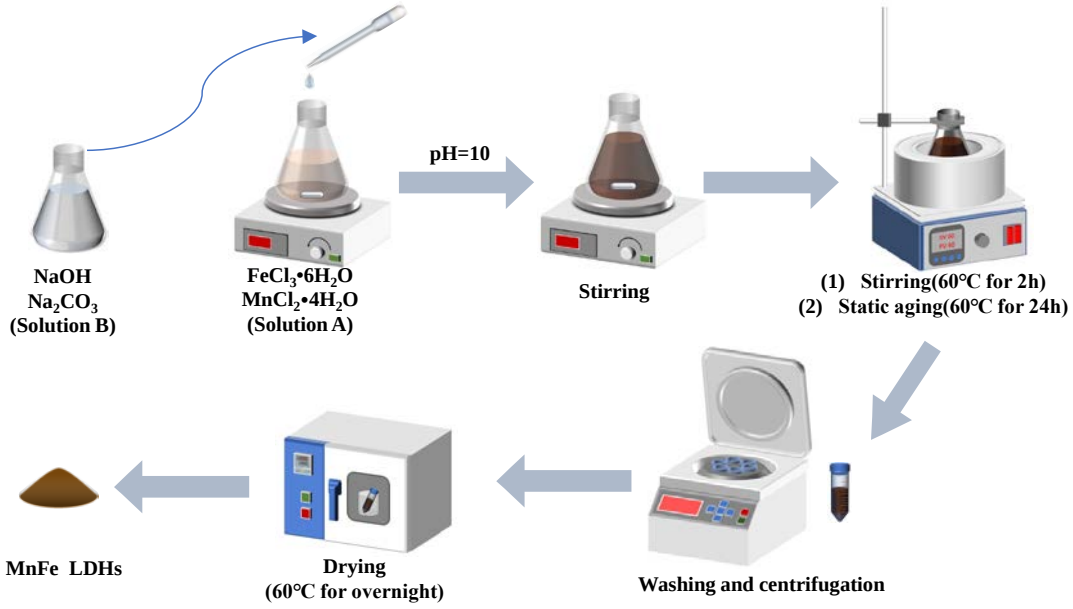

Fig. S1 Schematic diagram of the production process of MnFe-LDH.

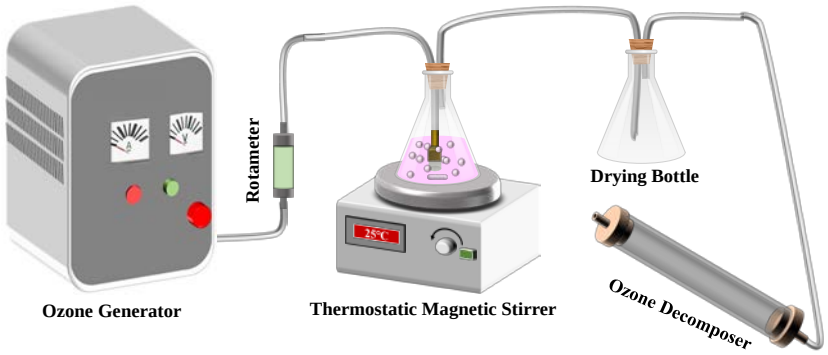

Fig. S2 Schematic diagram of the experimental setup.

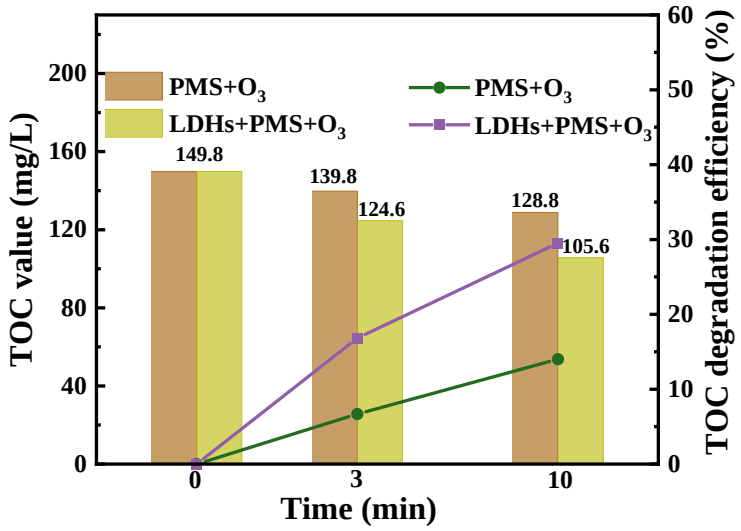

Fig. S3 TOC values and TOC removal rates in PMS/O_3 and MnFe-LDH/PMS/O_3 degradation RhB reaction systems. (Reaction conditions: $[MnFe\text{-}LDH]_0$ = 0.4 g/L, $[PMS]_0$ = 0.2 g/L, $[O_3]_0$ = 0.3 L/min, pH = 5.71 (unadjusted)).

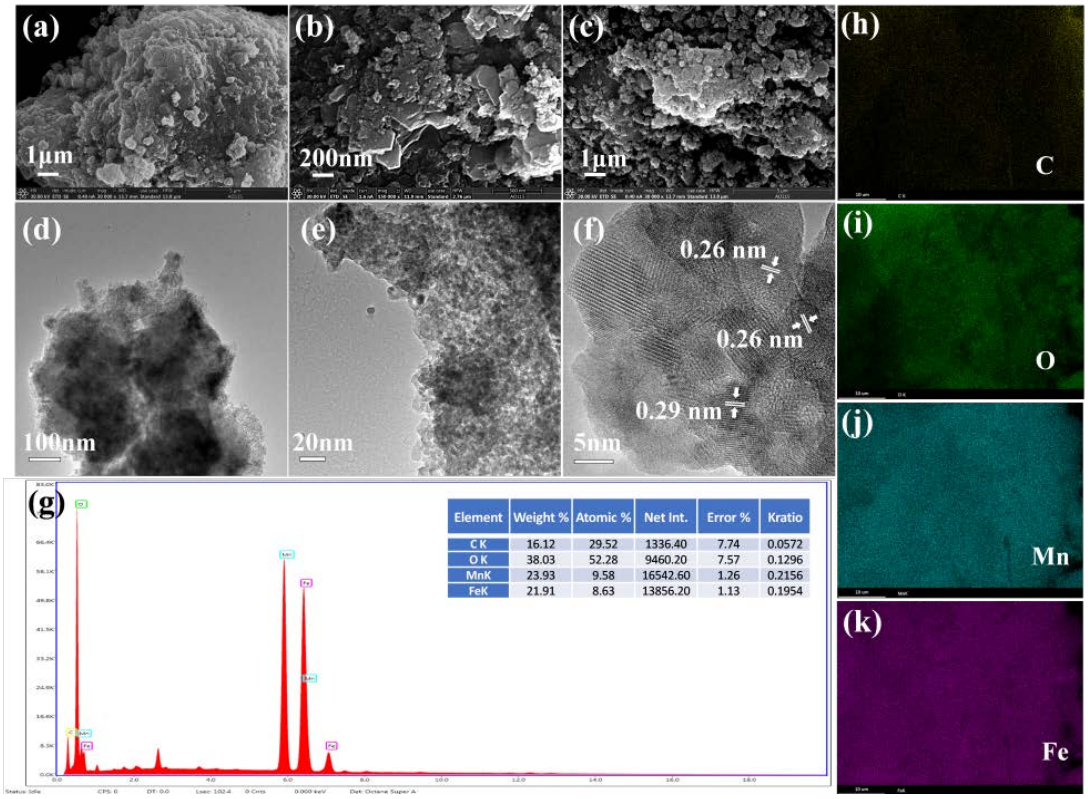

Fig. S4 SEM pictures of MnFe-LDH before reaction (a, b) and after recycling (c), TEM pictures (d, e, f), EDS (g) and Mapping (h–k) of MnFe-LDH.

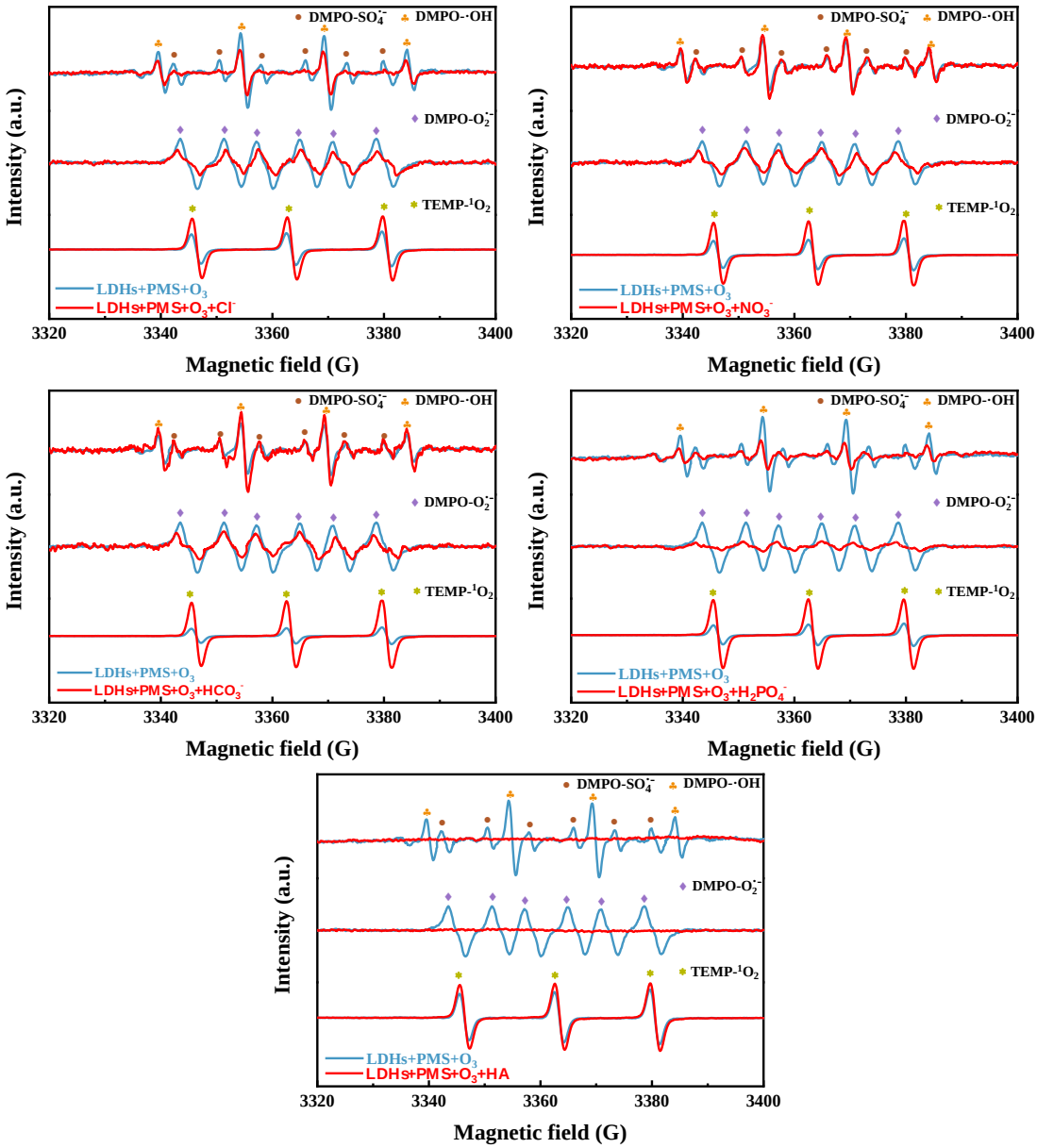

Fig. S5 EPR spectra in the presence of different anions: Cl^- (a), NO_3^- (b), HCO_3^- (c), $H_2PO_4^-$ (d), and HA (e). (Reaction conditions: $[MnFe\text{-}LDH]_0$ = 0.4 g/L, $[PMS]_0$ = 0.2 g/L, $[O_3]_0$ = 0.3 L/min, pH = 5.71 (unadjusted)).

Text S1 Equations of reactions

$$HSO_5^- \rightarrow SO_5^{2-} + H^+ \quad (S1)$$

$$SO_5^{2-} + O_3 \rightarrow SO_8^{2-} \quad (S2)$$

$$SO_8^{2-} \rightarrow SO_5^{\bullet-} + O_3^{\bullet-} \quad (S3)$$

$$SO_5^{\bullet-} + O_3 \rightarrow SO_4^{\bullet-} + 2O_2 \quad (S4)$$

$$2SO_5^{\bullet-} \rightarrow 2SO_4^{\bullet-} + O_2 \quad \text{(S5)}$$

$$2SO_5^{\bullet-} \rightarrow S_2O_8^{2-} + O_2 \quad \text{(S6)}$$

$$O_3^{\bullet-} + H^+ \rightarrow HO_3^{\bullet} \quad \text{(S7)}$$

$$O_3^{\bullet} \rightarrow O_2 + \bullet OH \quad \text{(S8)}$$

$$SO_4^{\bullet-} + H_2O \rightarrow H^+ + SO_4^{2-} + \bullet OH \quad \text{(S9)}$$

$$SO_4^{\bullet-} + OH^- \rightarrow SO_4^{2-} + \bullet OH \quad \text{(S10)}$$

$$HSO_5^- + \bullet OH \rightarrow SO_5^{\bullet-} + H_2O \quad \text{(S11)}$$

$$HSO_5^- + SO_4^{\bullet-} \rightarrow SO_5^{\bullet-} + HSO_4^- \quad \text{(S12)}$$

$$SO_4^{\bullet-} + \bullet OH \rightarrow 1/2O_2 + HSO_4^- \quad \text{(S13)}$$

$$\bullet OH + H^+ + e^- \rightarrow H_2O \quad \text{(S14)}$$

$$SO_4^{\bullet-} + H^+ + e^- \rightarrow HSO_4^{\bullet-} \quad \text{(S15)}$$

$$SO_4^{\bullet-} + OH^- \rightarrow SO_4^{2-} + \bullet OH \quad \text{(S16)}$$

$$\bullet OH + Cl^- \rightarrow HClO^{\bullet-} \quad \text{(S17)}$$

$$SO_4^{\bullet-} + Cl^- \rightarrow Cl\bullet + SO_4^{2-} \quad \text{(S18)}$$

$$Cl\bullet + Cl^- \rightarrow Cl_2^{\bullet-} \quad \text{(S19)}$$

$$O_3^- \rightarrow NO_2^- + O_2 \quad \text{(S20)}$$

$$NO_3^- \rightarrow NO_2\bullet + O^{\bullet-} \quad \text{(S21)}$$

$$O^{\bullet-} + H_2O \rightarrow \bullet OH + OH^- \quad \text{(S22)}$$

$$SO_4^{\bullet-} + H_2PO_4^- \rightarrow SO_4^{2-} + PO_4^{\bullet-} + H^+ \quad \text{(S23)}$$

$$\bullet OH + H_2PO_4^- \rightarrow H_2O + PO_3^{\bullet-} \quad \text{(S24)}$$

Text S2 Materials and reagents

Manganese chloride ($MnCl_2$•$4H_2O$), ferric chloride ($FeCl_3$•$6H_2O$), sodium thiosulphate pentahydrate ($Na_2S_2O_3$•$5H_2O$), hydrochloric acid (HCl), sodium hydroxide (NaOH), potassium nitrate (KNO_3), methanol (MeOH), ethanol (EtOH), tert-butanol (TBA), and Rhodamine B (RhB) were purchased from Damao Chemical Reagent Co. Ltd (Tianjin, China). Sodium carbonate anhydrous (Na_2CO_3), sodium azide (NaN_3), and potassium chloride (KCl) were supplied by Sinopharm Holdings Chemical Reagent Co. Ltd (Shanghai, China). Peroxymonosulfate (PMS, $KHSO_5$•$0.5KHSO_4$•$0.5K_2SO_4$) and p-benzoquinone (p-BQ) were obtained from Aladdin Chemical Co. Ltd (Shanghai, China). Potassium bicarbonate ($KHCO_3$) was achieved from Kermel Chemical Reagent Co. Ltd (Tianjin, China). Potassium phosphate (K_2HPO_4) was acquired from Guangfu

Chemical Reagent Co. Ltd (Tianjin, China). All chemicals are analytical grade and can be used without further purification. In addition, deionized water (DI) was used throughout the experiments.

Text S3 Characterizations

The surface morphology, elemental composition, and microstructure of the samples were characterized by Scanning Electron Microscopy (SEM, Apreo S, Thermo, USA) and Transmission Electron Microscopy (TEM, Tecnai F30, FEI, Netherlands). The crystal structure of the samples was characterized by X-ray Diffractometry using focused light in the 2θ range of 10°–80° (XRD, UltimaIV, Rigaku, Japan). X-ray Photoelectron Spectroscopy (XPS, Kratos Axis Ultra Dld, Kratos, UK) tests use Al Kα as the X-ray source (hv = 1486.6 eV) in steps of 0.05 eV to scan full and fine spectra of samples to study elemental changes on the surface of the material. The Raman spectra of the catalysts were recorded using a confocal Raman spectroscopy (Raman, WITec alpha 300 R, WITec, Germany). The samples are characterized using Fourier Transform Infrared Spectroscopy (FT-IR, Nexus 670, Nicolet, UAS) in the range 400–4000 cm^{-1} to analyze the presence and changes in functional groups or chemical bonds on the surface of the material. The pH_{pzc} corresponding to the zero-point charge on the catalyst surface was determined using a Zeta Potential and Particle Size Analyzer (Zeta, 90Plus Pals, Brookhaven, USA). The specific surface area and pore size of the catalysts were determined using a fully automated specific surface area physisorption instrument (BET, ASAP2020M, Micromeritics, USA). The absorbance of rhodamine B was determined at 550 nm using an Ultraviolet-visible Spectrophotometer (UV-Vis, Evolution 300, Thermo Fisher, USA). The main reactive oxygen species during the reaction were identified using Electron Paramagnetic Resonance Spectrometry (EPR, ER200DSRC10/12, Bruker, Germany). The intermediate products of RhB degradation were identified by Liquid Chromatography-Mass Spectrometry (LC-MS, Thermos TSO Quantum Ultra, Thermo Fisher, USA). Metal precipitation in the water samples was measured using plasma emission spectrometry (ICP, Plasma Quant PQ9000, Analytikjena, Germany).

Text S4 Identification of reactive free radicals

1) Free radical burst assay

Tert-Butanol (TBA), Isopropyl Alcohol (IPA), p-Benzoquinone (p-BQ) and Sodium Azide (NaN_3) were used as radical bursting agents for •OH, •OH and $SO_4^{\bullet-}$, $O_2^{\bullet-}$, and $^1O_2$, respectively, which investigated the free radicals generated during the reaction and the extent of their contribution.

The univariate approach was used in the experiment. Before degradation, quenchers were added to the solution respectively, and then catalyst and PMS were added for the degradation experiment to explore the influence on pollutant degradation.

2) Electron paramagnetic resonance spectroscopy

The main reactive oxygen species produced in the catalytic system were detected using Electron Paramagnetic Resonance (EPR) spectroscopy. 5,5-dimethyl-1-pyrroline-N-oxide (DMPO) was used in water and methanol to capture •OH and $SO_4^{\bullet-}$, and $O_2^{\bullet-}$. 4-amino-2,2,6,6-tetramethylpiperidine (TEMP) was used to capture $^1O_2$. The experimental procedure was as follows.

After aeration with ozone in 50 mL of deionized water or methanol for 10 min, the prepared MnFe-LDH and PMS were placed in the aeration beaker and stirred uniformly for 1 min. An appropriate amount of the solution was filtered through a 0.22 μm filter membrane and placed in a centrifuge tube. Then, 1 mL sample solution was taken with a pipette and transferred to a centrifuge tube. 11 μL DMPO or 17 μL TEMP was added to form the additional product. The sample then was aspirated with a capillary tube to more than half the length of the column, and the lower end of the capillary tube was calcined with a flame to make it sealed. Finally, the capillary is placed in a quartz injection tube and placed in the sample chamber of the tester for testing. Different bursting agents can be added as required for different test situations.

Text S5 Identification of degradation products

A liquid chromatography-mass spectrometer (LC-MS) was used to identify the oxidative degradation intermediates of the target contaminants as a means to infer the possible degradation pathways of the contaminants. The degradation intermediates were determined using a Welch Ultimate C18 column (2.1 × 100 mm, 3 um) at a flow rate of 0.2 mL/min. RhB was measured in positive electrospray ionization (EIS^+) mode, running in full scan mode over a range of 50–1000 m/z.

Text S6 Catalyst recovery process

The remaining material in the solution was recovered by high-speed centrifugation at the end of the degradation experiment and washed several times with ethanol and deionized water

respectively. The washed material was dried in an oven at 60℃ and then used for subsequent reproducibility experiments.

Table S1 Intermediates generated during the RhB degradation by MnFe-LDH/PMS/O_3 system.

No.	m/z	Molecular formula	Structural formula
RhB	443	$C_{28}H_{32}N_2O_3$	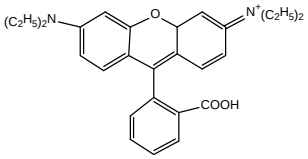
P1	415	$C_{26}H_{27}N_2O_3$	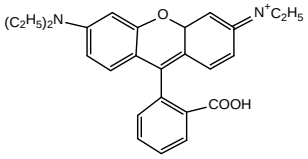
P2	415	$C_{26}H_{27}N_2O_3$	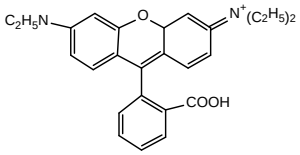
P3	387	$C_{24}H_{23}N_2O_3$	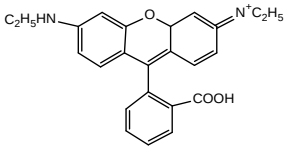
P4	387	$C_{24}H_{24}N_2O_3$	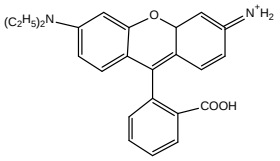
P5	387	$C_{24}H_{24}N_2O_3$	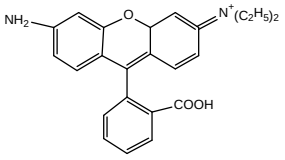
P6	359	$C_{22}H_{19}N_2O_3$	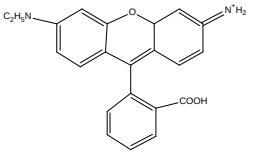
P7	359	$C_{22}H_{19}N_2O_3$	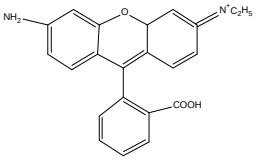
P8	332	$C_{20}H_{16}N_2O_3$	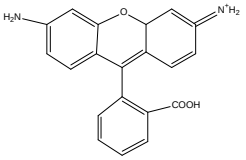

P9	258	$C_{19}H_{14}O$	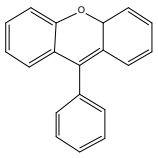
P10	276	$C_{18}H_{12}O_3$	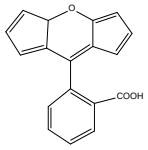
P11	220	$C_{17}H_{16}$	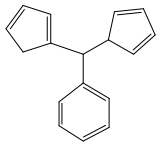
P12	138	$C_7H_6O_3$	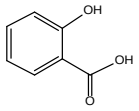
P13	110	$C_6H_6O_2$	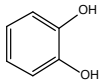
P14	160	$C_7H_{12}O_4$	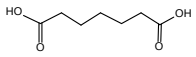
P15	146	$C_6H_{10}O_4$	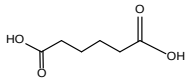
P16	74	$C_3H_6O_2$	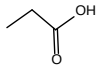

Table S2 The acute toxicity, developmental toxicity, and mutagenicity of RhB and its degradation intermediates.

No.	Fathead minnow (LC_{50} 96h)	Daphnia (LC_{50} 48h)	Developmental Toxicity value	Mutagenicity value
RhB	0.0393	4.63	0.95	0.26
1	0.0368	4.19	0.94	0.37
2	0.0468	9.6	1.03	0.43
3	0.14	7.19	0.89	0.4
4	0.31	72.19	0.92	0.5
5	0.27	8.4	0.83	0.34
6	0.55	66.75	1.1	0.39
7	0.26	5.21	0.84	0.34
8	0.51	38.05	1.2	0.46
9	0.1	1.02	0.69	0.62
10	0.15	8.42	0.98	0.3
11	0.5	0.3	0.98	0
12	98.34	84.61	0.2	0
13	41.2	11.58	0.54	0.48
14	147.91	167.6	0.39	0.7
15	90.56	114.89	0.74	0.26
16	206.36	205.83	0.77	0